Pesticide Biochemistry and Physiology 213 (2025) 106471

Contents lists available at ScienceDirect

Pesticide Biochemistry and Physiology

journal homepage: www.elsevier.com/locate/pest

The sustainable fungicide choline pelargonate inhibits *Botrytis cinerea* and *Phytophthora infestans* growth by altering membrane structure and lipid content

Sofia Montanari [a,b], Francesco Trenti [c], Andrea Nesler [d], Lorella Navazio [e,f], Barbara Baldan [e,f], Graziano Guella [c], Claudia M.O. Longa [b], Michele Perazzolli [a,b,*]

[a] Center Agriculture Food Environment (C3A), University of Trento, Via E. Mach 1, 38098 San Michele all'Adige, Trento, Italy
[b] Research and Innovation Centre, Fondazione Edmund Mach, Via E. Mach 1, 38098 San Michele all'Adige, Trento, Italy
[c] Department of Physics, University of Trento, Via Sommarive 14, 38123 Povo, Trento, Italy
[d] Bi-PA nv (Biological Products for Agriculture), Technologielaan 7, 1840 Londerzeel, Belgium
[e] Department of Biology, University of Padova, Via U. Bassi 58/B, 35131 Padova, Italy
[f] Botanical Garden, University of Padova, Via Orto Botanico 15, 35123 Padova, Italy

ARTICLE INFO

Keywords:
Choline carboxylates
Fungicide
Grey mold
Late blight
Membrane disruption

ABSTRACT

Botrytis cinerea and *Phytophthora infestans* are two of the most widespread phytopathogens worldwide and are mainly controlled by the frequent application of synthetic chemical fungicides. Sustainable alternatives are required to reduce the possible negative effects on human health and the environment. This study aimed to characterize the mechanism of action of the sustainable fungicide choline pelargonate (CP) against *B. cinerea* and *P. infestans in vitro*. CP inhibited mycelial growth and spore germination of *B. cinerea* and *P. infestans*, causing the leakage of electrolytes and nucleic acids with dose-dependent effects. Ultrastructural alterations of the plasma membrane and cytoplasm were found in *B. cinerea* and *P. infestans* cells, with negative impacts on membrane functionality. Moreover, CP altered the content of free fatty acid, phosphatidic acid, phosphatidylcholine, phosphatidylethanolamine, and triglyceride lipid classes in *B. cinerea* and *P. infestans* mycelia, as a possible perturbation of lipid metabolism and stimulation of lipid hydrolysis. Pelargonic acid was partially incorporated into triglyceride lipids, suggesting attempted detoxification mechanisms in both phytopathogens. In conclusion, CP is a choline carboxylate with promising inhibitory activity against phytopathogens.

1. Introduction

Botrytis cinerea and *Phytophthora infestans* are two of the most widespread phytopathogens worldwide (Judelson, 2014; Williamson et al., 2007). *Botrytis cinerea* is a necrotrophic phytopathogen that causes grey mold disease on different plant organs (e.g., flowers, fruits, leaves, shoots, and soil storage organs) of more than 500 plant species, such as vegetable crops (e.g., cucumber, tomato, and zucchini) and fruit-bearing plants (e.g., grape, raspberry, and strawberry) with high economic relevance (Cheung et al., 2020). The ascomycete *B. cinerea* primarily propagates through asexual conidia, and its alternative sources of infection are mycelia from sclerotia and infected tissues (Cheung et al., 2020). Moreover, *B. cinerea* undertakes a sexual cycle to form apothecia that release ascospores, although infections by ascospores rarely occur in nature (Cheung et al., 2020). *Botrytis cinerea* is most destructive on mature and senescent tissues of dicotyledonous hosts, but it usually infects plant tissues at early stages and remains quiescent before rotting the infected tissues, when the host physiology changes and environmental conditions are conducive for pathogen development (Williamson et al., 2007). In particular, *B. cinerea* causes soft rots, accompanied by collapse and water-soaking of parenchyma tissues, with a rapid appearance of grey masses of conidia (Williamson et al., 2007). *Phytophthora infestans* is a hemibiotrophic oomycete responsible for tomato and potato late blight that predominantly follows asexual reproduction through sporangia formation during the growing season (Judelson, 2014). Asexual sporangia may directly extend hyphae through the sporangial wall (direct germination) or release mononucleate zoospores (indirect germination) (Judelson and Blanco, 2005), while oospores can

* Corresponding author at: Center Agriculture Food Environment (C3A), University of Trento, Via E. Mach 1, 38098 San Michele all'Adige, Trento, Italy.
E-mail address: michele.perazzolli@unitn.it (M. Perazzolli).

https://doi.org/10.1016/j.pestbp.2025.106471
Received 5 December 2024; Received in revised form 30 April 2025; Accepted 22 May 2025
Available online 29 May 2025

originate from sexual reproduction (Judelson, 2014). The main symptoms of tomato late blight include the formation of black/brown lesions on leaves, fruits, and stems that progress to water-soaked chlorotic spots, which can lead to necrosis of the entire plant (Mazumdar et al., 2021). Moreover, symptoms of potato late blight include blight or brown rot on tubers and water-soaked lesions on leaves, often surrounded by white areas of sporulation (Yuen, 2021).

Botrytis cinerea and *P. infestans* infections cause severe crop losses worldwide (Abbey et al., 2019; Nowicki et al., 2012), and disease management strategies are commonly applied against these two pathogens, such as the use of chemical fungicides, resistant cultivars, and agronomic practices (Abbey et al., 2019; Mazumdar et al., 2021). Chemical fungicides are the most important approach for *B. cinerea* control (Abbey et al., 2019), and they can be differentiated according to their modes of action, such as multi-site fungicides (e.g., captan, chlorothalonil, dichlofluanid, folpet, mancozeb, and tolylfluanid), uncouplers of oxidative phosphorylation (e.g., fluazinam), inhibitors of mitochondrial respiration (e.g., azoxystrobin and other strobilurins, boscalid and other carboxamides), and perturbators of osmoregulation (e.g., dicloran, fenpiclonil, fludioxonil, and quintozene) (Leroux, 2007). Likewise, fungicides used against *P. infestans* include site-specific products (e.g., azoxystrobin, cyazofamid, fluazinam, mandipropamid, metalaxyl, and oxathiapiprolin) or multi-site products (e.g., copper and sulfur) (Ivanov et al., 2021). It was estimated that a large fraction of the global fungicide market is used to control *B. cinerea* (Abbey et al., 2019) and that chemical control of *P. infestans* contributes to 10–20 % of the total production costs of potato in Europe and the U.S.A. (Haverkort et al., 2009). However, the overuse of chemical fungicides raised concerns about possible residues on fruits and vegetables with consequent negative effects on human health and the environment (Abbey et al., 2019). Because of these concerns, regulations have been implemented in several countries to reduce the use of chemical fungicides (Skevas et al., 2013). For example, maneb and mancozeb, previously used against *B. cinerea* (Leroux, 2007) and *P. infestans* (Ivanov et al., 2021), are no longer allowed in Europe (https://food.ec.europa.eu/plants/pesticides/eu-pesticides-database_en). Numerous active substances are under scrutiny for substitution in Europe, including those used against *B. cinerea* and/or *P. infestans*, such as boscalid, copper, and metalaxyl (Commission, E, 2015). Likewise, copper use is limited in Europe up to a maximum of 28 kg/ha over a period of seven years (Commission, E, 2018) and further limitations are expected in the future (Tamm et al., 2022). Thus, the development of novel sustainable fungicides is of great importance to reduce the health risks and environmental impacts (Tleuova et al., 2020).

Choline pelargonate (CP; also known as trimethyl-ethanolamine nonanoate or choline nonanoate) is a new formulation of pelargonic acid as choline salt for the use as a sustainable fungicide against fungal and oomycete phytopathogens (De Saegher et al., 2019). For example, CP treatment successfully controlled late blight on potato leaves and powdery mildew (caused by *Podosphaera xanthii*) on zucchini plants (De Saegher et al., 2019). Pelargonic acid (also known as nonanoic acid) is a saturated free fatty acid (FFA) with nine carbon atoms (Δ9:0), naturally present at low concentrations in fruits, vegetables, milk, and beef (Ciriminna et al., 2019). Pelargonic acid is used as bio-based herbicide in concentrated formulations (Ciriminna et al., 2019) and showed antimicrobial activities against human pathogens, such as *Salmonella enterica* subsp. *enterica* (Dev Kumar et al., 2020) and *Microsporum gypseum* (Chadeganipour and Haims, 2001). Choline, the other component of CP, is considered safe by the Food and Drug Administration (U.S.A.) and the European Food Safety Agency (Li et al., 2022), and it is a micronutrient involved in many physiological pathways of human cells (Penry and Manore, 2008). CP belongs to the subclass of ionic liquids named choline carboxylates, which include biocompatible substances that interact with bilayer membranes of liposomes when the chain length contains more than eight carbon atoms (Rengstl et al., 2014). Chemical characteristics and possible applications of choline carboxylates were partially evaluated as solvents in the cosmetic, food, and pharmaceutical industries (Elhi et al., 2020; Rengstl et al., 2014), but no information is available on the possible effect of CP against phytopathogens. This study aimed to understand the mechanism of action of CP against *B. cinerea* and *P. infestans in vitro* by investigating possible perturbations of membrane structure and lipid content.

2. Materials and methods

2.1. Biological material, growth conditions, and treatments

Botrytis cinerea B05.10 (Amselem et al., 2011) and *P. infestans* VB3 (Chahed et al., 2020) were grown in Petri dishes on potato dextrose agar (PDA; 4 g/L potato extract, 20 g/L dextrose, 15 g/L agar; Oxoid, Basingstoke, Hampshire, UK) and pea agar medium (PAM, 125 g/L frozen peas and 12 g/L agar in distilled water) (Puopolo et al., 2014) at 18 ± 2 °C in the dark, respectively.

The stock solution of CP [41 % (*w/v*); CAS number 10246–69-2] was provided by Bi-PA nv. (Londerzeel, Belgium).

2.2. Assessment of choline pelargonate impact on B. cinerea and P. infestans mycelial growth

The inhibitory activity of CP on *B. cinerea* and *P. infestans* mycelial growth was assessed as previously described (Chahed et al., 2020). Briefly, *B. cinerea* and *P. infestans* plugs (5 mm diameter) were cut from the edge of seven-day-old colonies and a plug was placed at the center of a dish (90 mm diameter) on PDA and PAM supplemented with the appropriate CP concentration (0, 0.1, 0.5, 1.0, 1.5, 2.0, 3.0, and 5.0 mM), respectively. The mycelial growth of *B. cinerea* and *P. infestans* was assessed after four and eleven days of incubation at 18 ± 2 °C in the dark, respectively, and it was calculated as the average of the two perpendicular diameters of the colony, minus the plug diameter. The percentage of mycelial growth inhibition was calculated according to the following equation: (colony diameter in control dishes - colony diameter in CP-treated dishes) / colony diameter in control dishes × 100 (Yahyazadeh et al., 2008). The concentration that inhibited 50 % of mycelial growth (IC50) was calculated according to the regression curve of mycelial growth against the Log_{10}-transformed CP concentration. When no mycelial growth was observed, CP-treated *B. cinerea* and *P. infestans* plugs were transferred to new PDA and PAM dishes, respectively, and radial growth was monitored for three days of incubation at 18 ± 2 °C in the dark to assess mycelial vitality. The minimum CP concentration that completely inhibited (100 % growth inhibition) the mycelial growth and allowed mycelial growth (vital mycelium) when transferred to a new PDA (for *B. cinerea*) or PAM (for *P. infestans*) dish was defined as minimum inhibitory concentration (MIC) (Zhang et al., 2019). The minimum CP concentration that completely inhibited (100 % growth inhibition) the mycelial growth and avoided mycelial growth (death mycelium) when transferred to a new PDA (for *B. cinerea*) or PAM (for *P. infestans*) dish was defined as minimum fungicidal concentration (MFC) (Zhang et al., 2019). Six replicates (dishes) were analyzed for each CP concentration and phytopathogen, and the experiment was carried out twice.

2.3. Assessment of choline pelargonate impact on the germination of B. cinerea conidia and P. infestans sporangia

The inhibitory activity of CP on the germination of *B. cinerea* conidia and *P. infestans* sporangia was assessed according to Song et al. (2016). Briefly, two-week-old *B. cinerea* and three-week-old *P. infestans* dishes were filled with 4 mL of sterile distilled water and gently scraped with a sterile L-shaped loop to collect conidia and sporangia, respectively. The resulting spore suspension was filtered using a sterile Pasteur pipette containing a fine muslin cloth, the concentration was determined by using a hemocytometer under a light microscope (Eclipse 80i, Nikon,

Tokyo, Japan), and spore suspension was subsequently diluted with sterile distilled water to obtain a concentration of 1×10^6 spores/mL. An aliquot (50 μL) of *B. cinerea* conidial and *P. infestans* sporangial suspension was spread on water agar (WA; 15 g/L agar) and PAM dishes supplemented or not (control) with CP at the concentrations corresponding to IC50, MIC, and MFC, respectively. *Botrytis cinerea* and *P. infestans* germination was assessed by counting 100 conidia and sporangia for each dish under the light microscope after 24 h and 48 h of incubation at 18 ± 2 °C in the dark, respectively. Conidia and sporangia were considered germinated when the germ tube length was at least half the spore diameter (Song et al., 2016). The percentage of germination inhibition was calculated according to the following equation: (germinated spores in control dishes - germinated spores in treated dishes) / germinated spores in control dishes × 100. Six replicates (dishes) were analyzed for each CP concentration and phytopathogen, and the experiment was carried out twice.

2.4. Assessment of choline pelargonate effects against B. cinerea on tomato plants under greenhouse conditions

The efficacy of CP against *Botrytis cinerea* was assessed as previously described by Baccelli et al. (2022) with slight modifications. Briefly, tomato seedlings (*Solanum lycopersicum* L. cultivar Moneymaker) were grown for four weeks in pots (70 mL) containing a mixture of brown and blonde peat (Semina 80, Tercomposti, Calvisano, Italy) under greenhouse conditions with a photoperiod of 16 h light and 8 h dark at 25 ± 1 °C and 70 ± 10 % relative humidity (RH). All leaves of each plant were treated with water (control), 2.0 mM, 8.0 mM, or 16.0 mM CP using a hand sprayer (5–10 mL for each plant). One day after treatment, plants were inoculated with the *B. cinerea* conidial suspension (1×10^6 spores/mL) using a hand sprayer (5–10 mL for each plant) and incubated for 48 h under greenhouse conditions at 98 ± 2 %RH. The disease severity of each plant was visually assessed as the percentage of leaf area covered by necrosis (Baccelli et al., 2022). Eight replicates (plants) were used for each treatment, and the experiment was carried out twice.

2.5. Assessment of choline pelargonate impact on B. cinerea and P. infestans membrane permeability

Botrytis cinerea and *P. infestans* mycelia were grown for seven days and 14 days on PDA and PAM dishes covered with sterile cellophane layers, respectively. The separate mycelial cultures were then transferred to a 50 mL-tube and incubated in 40 mL of sterile distilled water supplemented or not (control) with CP at the concentrations corresponding to IC50, MIC, and MFC at 18 ± 2 °C in the dark under orbital shaking at 120 rpm. To assess the leakage of electrolytes, the electrical conductivity of each solution was analyzed after 0 h, 8 h, 24 h, and 48 h of incubation using a conductivity meter (VWR pH CO 1030, VWR, Radnor, Pennsylvania, U.S.A.) as previously described (Li et al., 2016). Samples were autoclaved, and electrical conductivity was assessed after equilibration at room temperature. Electrolyte leakage (%) of each sample was calculated for each time point according to the following equation: (electrical conductivity at time point t / electrical conductivity after autoclave treatment) × 100.

To assess the leakage of nucleic acids, an aliquot (1 mL) of each solution was collected after 0 h, 8 h, 24 h, and 48 h of incubation or after autoclave treatment, and the optical density at 260 nm (OD_{260}) was assessed using a spectrophotometer (Ultrospec 3100 Pro, Amersham Biosciences, Amersham, UK) (Chen et al., 2020). The leakage of nucleic acids (%) of each sample was calculated for each time point according to the following equation: (OD_{260} at time point t / final OD_{260} after autoclave treatment) × 100.

Six replicates (tubes) were analyzed for each CP concentration, phytopathogen, and time point, and the experiment was carried out twice.

2.6. Sample collection for ultrastructural and lipid analyses

Seven-day-old *B. cinerea* and 14-day-old *P. infestans* dishes were filled with 4 mL of potato dextrose broth (PDB; 4 g/L potato extract, 20 g/L dextrose; Oxoid) and pea broth (PB; 125 g/L frozen peas in distilled water), respectively, and gently scraped with a sterile L-shaped loop to collect mycelial fragments. Each *B. cinerea* and *P. infestans* suspension (500 μL) was inoculated in 25 mL PDB and PB in a 50 mL-tube, respectively, and mycelial cultures were incubated for 5 days at 18 ± 2 °C in the dark under orbital shaking at 120 rpm.

For ultrastructure analyses, water (control) or CP was added at the concentrations corresponding to IC50 and MFC, and mycelial cultures were collected after 8 h and 48 h of incubation at 18 ± 2 °C in the dark under orbital shaking at 120 rpm.

For lipid analyses, mycelial cultures were washed three times with sterile distilled water by centrifugation at 4000 ×*g* for 10 min at room temperature and resuspended in 40 mL of sterile distilled water supplemented or not (control) with CP at the concentrations corresponding to IC50 and MFC. After 48 h of incubation at 18 ± 2 °C in the dark under orbital shaking at 120 rpm, mycelial samples (2 g) from each replicate (tube) were collected and immediately frozen in liquid nitrogen. Mycelial samples were ground using a mixer-mill disruptor (MM 400, Retsch, Haan, Germany) with refrigerated stainless jars at 25 Hz for 30 s, and the resulting mycelium powder was stored at −80 °C.

CP concentrations and time points were selected according to the results of electrolyte and nucleic acid leakage, and three replicates (tubes) were analyzed for each CP concentration, phytopathogen, and time point.

2.7. Sample fixation and ultrastructural analysis by transmission electron microscopy (TEM)

Ultrastructural analysis of *B. cinerea* and *P. infestans* was carried out as previously described (Chahed et al., 2020). Briefly, each mycelial sample (0.5 cm^3) was incubated in 4 mL of fixing solution (3 % glutaraldehyde in 0.1 M cacodylate buffer, pH 7.4) for 1 h at room temperature under rotary shaking at 15 rpm and then overnight at 4 °C (Zuppini et al., 2010). Samples were washed three times in 500 mL of cacodylate buffer (0.1 M, pH 7.4), post-fixed for 2 h with 1 % (*w/v*) osmium tetroxide in 0.1 M cacodylate buffer (pH 7.4), and dehydrated in graded ethanol series of 25 %, 50 %, 75 %, and 100 % (*v*/v) with an incubation of 15 min at room temperature for each ethanol concentration. Samples were infiltrated in 1:3 (v/v) araldite resin/propylene oxide (Sigma-Aldrich, Merck, Rahway, NJ, U.S.A.) by incubation at 40 °C for 1 h, followed by incubation in 1:1 (v/v) araldite resin/propylene oxide at 40 °C for 1 h, and 3:1 (*v*/v) araldite resin/propylene oxide overnight at 40 °C. Samples were subsequently embedded in 100 % araldite resin by incubation at 40 °C for 24 h and at 60 °C for 72 h. Ultra-thin sections (70 nm) were obtained on a Reichert-Jung ultramicrotome (Leica Biosystems, Wetzlar, Germany) and mounted on uncoated copper grids. Sections were then stained with 1 % (v/v) uranyl acetate in 50 % (v/v) ethanol for 15 min and 1 % (v/v) lead citrate for 7 min. Observations were carried out with a Tecnai G2 transmission electron microscope (Field Electron and Ion Company, Hillsboro, OR, U.S.A.) operating at 100 kV and equipped with an Osis Veleta camera (Olympus, Tokyo, Japan).

2.8. Lipid extraction

Lipids were extracted according to the Folch method using a mixture of 2:1 (v/v) chloroform/methanol (Folch et al., 1957). Each ground mycelial sample (2 g of fresh weight) was resuspended in distilled water, and 2:1 (v/v) chloroform/methanol (7 mL) was then added. Each suspension was vortexed thoroughly and centrifuged at 6000 ×*g* for 10 min at room temperature to separate the two phases. The supernatant (organic phase) was collected, while the inter-layer sediment and the

aqueous phase were subjected to a second extraction with 7 mL of 2:1 (v/v) chloroform/methanol. After centrifugation at 6000 ×*g* for 10 min at room temperature, the organic phase was collected. For each sample, the organic phases obtained from the extraction were mixed and dried by N_2 flux to avoid oxidation. Dried lipid extracts of mycelial samples were weighted and stored at −80 °C until nuclear magnetic resonance (NMR) and high-performance liquid chromatography mass spectrometry (HPLC-MS) analyses.

2.9. Nuclear magnetic resonance (NMR) analysis of lipids

Each dried lipid extract was resuspended in 600 μL of a mixture of 9:1 (v/v) deuterated methanol (methanol-d_4)/deuterated chloroform, and NMR analysis was carried out as previously described (Novak et al., 2020). Briefly, ^{1}H NMR (400 MHz) and ^{31}P NMR (162 MHz) spectra were recorded at 26.85 °C on an NMR spectrometer (400 MHz, Bruker-Avance, Bremen, Germany), with a 5 mm double resonance broadband observe probe with pulsed-gradient field utility. The ^{1}H-90° proton pulse length was 9.3 μs, with a transmission power of 0 db. The ^{31}P-90° proton pulse length was 17 μs, with a transmission power of −3 db. The probe temperature was maintained at 26.85 °C using a variable temperature unit (B-VT 1000; Bruker). Calibration of the chemical shift scale (δ) was performed on the residual proton signal of methanol-d_4 at δ_H 3.310 ppm. The phosphatidylcholine (PC) signal at δ_P − 0.550 ppm was used to calibrate the ^{31}P NMR δ scale. The following measurements were performed: ^{1}H NMR as proton chemical shifts and scalar couplings, ^{31}P NMR composite pulse decoupling to remove any proton coupling in ^{31}P NMR spectra, where 4000 free induction decays were acquired and processed using exponential line broadening of 0.3 Hz before Fourier transformation. The resulting one-dimensional NMR spectra were analyzed using TopSpin 3.6.1 (Bruker, Bremen, Germany). The lipid classes from the NMR data were identified through comparisons with previous NMR measurements carried out with commercially available lipid standards. The molar fraction (percentage) of phosphatidic acid (PA), phosphatidylcholine (PC), and phosphatidylethanolamine (PE) lipid classes was assessed according to peak integration.

2.10. High-performance liquid chromatography-mass spectrometry (HPLC-MS) analysis of lipids

Each lipid extract was subjected to HPLC-MS analysis with a Model 1100 series instrument (Hewlett-Packard, Palo Alto, California, U.S.A.) using a quadrupole ion-trap mass spectrometer (Esquire LCTM; Bruker, Bremen, Germany) equipped with an electrospray ionization source in positive and negative ion modes, as previously described (Novak et al., 2020). Each dried lipid extract was resuspended in 1 mL of 9:1 (*v*/v) methanol/chloroform, and an aliquot (10 μL) was injected. Chromatographic separation was carried out at 29.85 °C with a thermostated C18 column (Kinetex 2.6 μm; 100 mm length, 2.6 μm particle size, 2.1 mm internal diameter, and 100 Å pore size; Phenomenex, Torrance, CA, U.S.A.) using 7:3 (v/v) methanol/H_2O containing 10 mM ammonium acetate (eluent A) and 1:9 (v/v) isopropanol/methanol containing 10 mM ammonium acetate (eluent B). Chromatographic separation of lipids was obtained with a linear elution gradient from 65 % eluent B to 100 % B in 40 min, and 20 min isocratic 100 % B at 1 mL/min. The column was re-equilibrated to 65 % B for 10 min. The MS scan range was 13,000 U/s from 50 to 1500 *m/z*, with a mass accuracy of 100 ppm. The nebulizer gas was high-purity nitrogen at a pressure of 20 to 30 psi, with a flow rate of 6 L/min at 300 °C. The electrospray ionization was operated in positive and negative ion modes for the qualitative and quantitative analyses of lipids. For the structural assignments of the lipid classes, extracted ion chromatograms from the positive and negative ion full scan data were integrated using the DataAnalysis 3.0 software (Bruker Daltonik, Bremen, Germany). Each FFA, PA, PE, PC, and triglyceride (TAG) lipid was named according to the number of carbon atoms and unsaturated bonds, and its content was expressed as peak area per ng of dried lipid extract (peak area/ng).

2.11. Statistical analysis

All experiments were carried out twice, and data were analyzed with R version 4.3.1. Normal distribution (Shapiro-Wilk test, $P > 0.05$) and variance homogeneity of the data (Levene tests, $P > 0.05$) were checked. Each experiment was analyzed individually, and the Kruskal-Wallis test was used to demonstrate non-significant ($P > 0.05$) experiment interaction (comparable results among experimental repetitions). Data from the two experiments were pooled, and normal distribution (Shapiro test, $P > 0.05$) and variance homogeneity (Levene test, $P > 0.05$) of the data were checked. Significant differences among treatments were assessed with the Kruskal-Wallis test ($P \leq 0.05$) followed by the Conovan-Iman test ($P \leq 0.05$).

3. Results

3.1. Choline pelargonate inhibited the mycelial growth and spore germination of B. cinerea and P. infestans, with leakage of electrolytes and nucleic acids

CP inhibited the mycelial growth of *B. cinerea* and *P. infestans* with dose-dependent effects (Fig. 1A), and IC50 values were 0.4 mM and 0.3 mM, respectively. MFC values corresponded to 2.0 mM for *B. cinerea* and 5.0 mM for *P. infestans,* while MIC value was 1.5 mM for both phytopathogens. CP inhibited the germination of *B. cinerea* conidia and *P. infestans* sporangia (Fig. 1B), and the inhibition percentages were 87.1 ± 3.7 % and 96.8 ± 0.9 % for *B. cinerea* (mean ± standard error), 98.9 ± 0.3 % and 99.8 ± 0.2 % for *P. infestans* at MIC and MFC dosages, respectively. Slight germination of *B. cinerea* conidia and *P. infestans* sporangia at MFC dosage suggested higher tolerance of spores compared to mycelia against CP. Moreover, CP decreased the severity of *B. cinerea* on tomato plants (Table 1).

To investigate CP impacts on *B. cinerea* and *P. infestans* membrane permeability, the leakage of electrolytes and nucleic acids was assessed. Electrolyte leakage was higher in CP-treated (IC50, MIC, and MFC dosages) compared to control *B. cinerea* and *P. infestans* mycelia immediately after CP addition (0 h) and after 8 h, 24 h, and 48 h of incubation (Fig. 2A and B). Moreover, electrolyte leakage was comparable among IC50, MIC, and MFC dosages after 24 h and 48 h of incubation of each phytopathogen. Dose-dependent effects of CP on the leakage of electrolytes were observed in *B. cinerea* and *P. infestans* mycelia after 8 h of incubation. Similarly, the leakage of nucleic acids was higher in CP-treated (IC50, MIC, and MFC dosages) compared to control mycelia after 24 h and 48 h of *B. cinerea* incubation, and after 8 h, 24 h, and 48 h of *P. infestans* incubation. Dose-dependent effects of CP on the leakage of nucleic acids were observed at 24 h and 48 h of *B. cinerea* and *P. infestans* incubation.

3.2. Choline pelargonate caused ultrastructural changes in B. cinerea and P. infestans cells

To investigate CP impacts on *B. cinerea* and *P. infestans* mycelia, ultrastructure analyses were carried out. A well-structured cell wall, intact plasma membrane, and regular organization of the cytoplasm and intracellular compartments (e.g., mitochondria and vacuoles) were observed in control *B. cinerea* and *P. infestans* cells (Fig. 3A-3D). Conversely, the structure of the cytoplasm and plasma membrane of *B. cinerea* and *P. infestans* cells was altered by CP treatment (Fig. 3E-3L). In *B. cinerea* cells, the plasma membrane was found to be detached from the cell wall, with cytoplasmic shrinkage and the establishment of plasmolysis after 48 h of incubation at IC50 dosage (Fig. 3E-3F). In *P. infestans* cells, an intense vacuolization was visible after 8 h and 48 h of incubation at IC50 dosage (Fig. 3G-3H). At MFC dosages, CP treatment caused severe alteration of the plasma membrane and

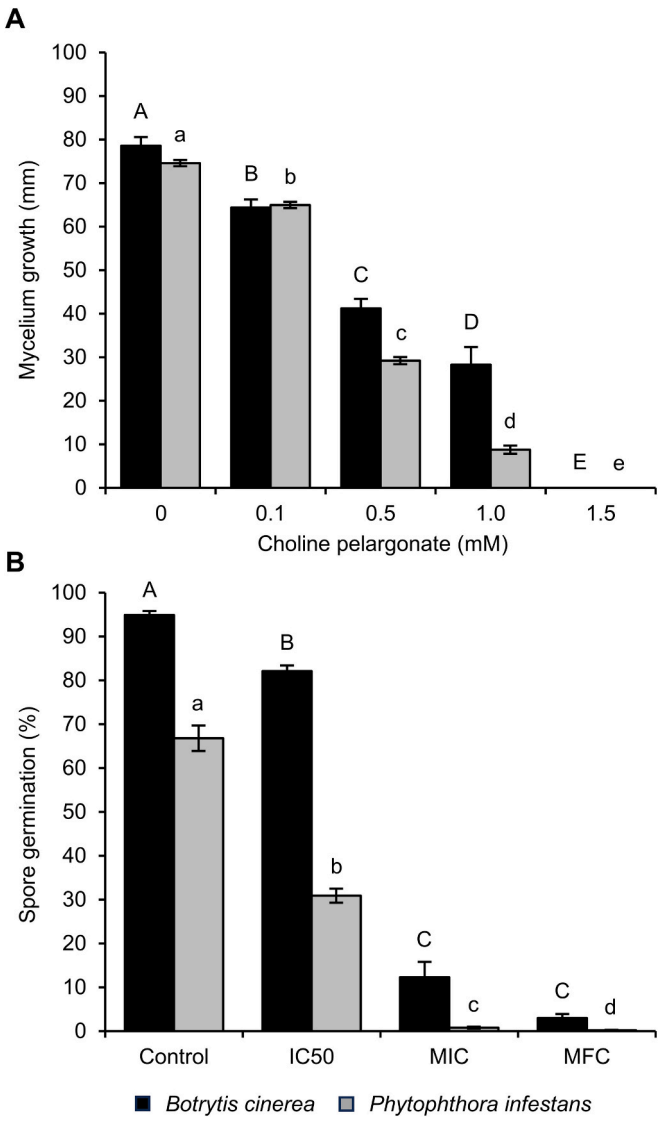

Fig. 1. Choline pelargonate inhibited the growth of *B. cinerea* and *P. infestans*. Mycelial growth (A) of *B. cinerea* (black) and *P. infestans* (grey) was assessed after four and eleven days of incubation on potato dextrose and pea agar medium supplemented with different choline pelargonate concentrations (mM), respectively. Germination percentage (B) of *B. cinerea* conidia (black) and *P. infestans* sporangia (grey) was assessed after 24 h and 48 h of incubation on water agar and pea agar medium supplemented or not (Control) with choline pelargonate at the concentration that inhibited 50 % of mycelial growth (IC50; 0.4 mM for *B. cinerea* and 0.3 mM *P. infestans*), minimum inhibitory concentration (MIC; 1.5 mM for *B. cinerea* and 1.5 mM *P. infestans*), and minimum fungicidal concentration (MFC; 2.0 mM for *B. cinerea* and 5.0 mM *P. infestans*), respectively. Comparable results were obtained between the two experiments (Kruskal-Wallis $P > 0.05$, six replicates per experiment), and data were pooled. Mean and standard error values of twelve replicates (dishes) from the two experiments are presented for each treatment. Different uppercase and lowercase letters indicate significant differences among treatments for *B. cinerea* and *P. infestans*, according to the Kruskal-Wallis test followed by the Conovan-Iman test ($P \leq 0.05$), respectively.

disorganization of the cytoplasm of *B. cinerea* and *P. infestans* after 8 h and 48 h of incubation (Fig. 3I-3L). In particular, shrunken cytoplasm and plasmolysis were observed in CP-treated *B. cinerea* cells already after 8 h of incubation (Fig. 3I), and the dismantling of the cytoplasm was found in CP-treated *P. infestans* cells after 48 h of incubation (Fig. 3L), with the leakage of cytoplasmic content in both phytopathogens.

Table 1
Choline pelargonate decreased *Botrytis cinerea* severity on tomato plants.

Treatment[a]	Disease severity (%)[b]
Control	43.9 ± 4.5 a
CP (2.0 mM)	38.2 ± 3.4 a
CP (8.0 mM)	18.9 ± 2.4 b
CP (16.0 mM)	5.5 ± 0.5 c

[a] Tomato plants were treated with water (Control), 2.0 mM, 8 mM, or 16 mM choline pelargonate (CP).
[b] *Botrytis cinerea* severity was assessed as the percentage of leaf area covered by leaf necrosis at 48 h post inoculation. Comparable results were obtained between the two experiments (Kruskal-Wallis $P > 0.05$, eight replicates per experiment), and data were pooled. Mean and standard error values of sixteen replicates (plants) from the two experiments are reported for each treatment. Different letters indicate significant differences among treatments, according to the Kruskal-Wallis test followed by the Conovan-Iman test ($P \leq 0.05$).

3.3. Choline pelargonate caused changes in *B. cinerea* and *P. infestans* lipid content

To verify CP impacts on *B. cinerea* and *P. infestans* lipid content, NMR and HPLC-MS analyses were performed. CP treatment altered phospholipid content of *B. cinerea* mycelia and ^{31}P NMR analysis showed a strong decrease of PA, PC, and PE lipid classes when applied at MFC dosage (Fig. 4A). Thus, the content of PA, PC, and PE lipids assessed by HPLC-MS analysis was lower in CP-treated (IC50 and MFC dosages) compared to control *B. cinerea* mycelia (Supplementary Fig. S1). In *P. infestans* mycelia, CP treatment decreased PA molar fraction, increased PC molar fraction, and slightly affected PE molar fraction (Fig. 4B), as a possible consequence of the perturbation of cellular membranes in both phytopathogens. In particular, the content of the most abundant PA [> 50 peak area/ng; PA (38:8; number of carbon atoms: number of unsaturated bonds), PA (38:9), and PA (40:9)] assessed by HPLC-MS analysis was comparable in CP-treated (IC50 and MFC dosages) and control *P. infestans* mycelia, while the content of PA (38:5) and PA (38:6) was higher in CP-treated (IC50 and MFC dosages) compared to control samples (Supplementary Fig. S2A). Moreover, PC (34:1), PC (34:2), PC (36:2), PC (36:3), and PC (38:6) were more abundant in CP-treated (IC50 and MFC dosages) compared to control samples, while PC (36:5), PC (38:5), PC (38:7), and PC (40:10) were not affected by CP treatment (Supplementary Fig. S2B). The content of PE (34:2) and PE (36:3) was not affected by CP treatment (IC50 and MFC dosages), while the content of PE (34,1) and PE (40,10) was higher and lower in CP-treated (MFC dosage) compared to control *P. infestans* mycelia, respectively (Supplementary Fig. S2C).

The content of TAG (52:3), TAG (52:4), and TAG (54:5) was lower in CP-treated (MFC dosage) compared to control *B. cinerea* mycelia (Fig. 5A). Moreover, TAG containing a lipophilic chain with nine carbon atoms were found in CP-treated (IC50 and MFC dosages) *B. cinerea* mycelia and they were not present in control samples, most likely due to the incorporation of pelargonic acid of CP in *B. cinerea* lipids. The content of FFA (16:0), FFA (18:0), FFA (18:1), FFA (18:2), FFA (18:3), was lower in CP-treated (IC50 and/or MFC dosages) compared to control samples as a possible perturbation of lipid metabolism and stimulation of lipid hydrolysis in *B. cinerea* mycelia (Fig. 5B). As expected, FFA (9:0) (corresponding to pelargonic acid) was found in CP-treated, but not in control, *B. cinerea* mycelia (Fig. 5B).

In *P. infestans*, the content of most abundant TAG (> 80 peak area/ng) was comparable in CP-treated (IC50 and MFC dosages) and control samples, such as TAG (54:3) TAG (58:3), and TAG (62:4) (Fig. 6A). TAG containing a lipophilic chain with nine carbon atoms were found in CP-treated (IC50 and MFC dosages) *P. infestans* mycelia and they were not present in control samples, as a possible incorporation of pelargonic acid

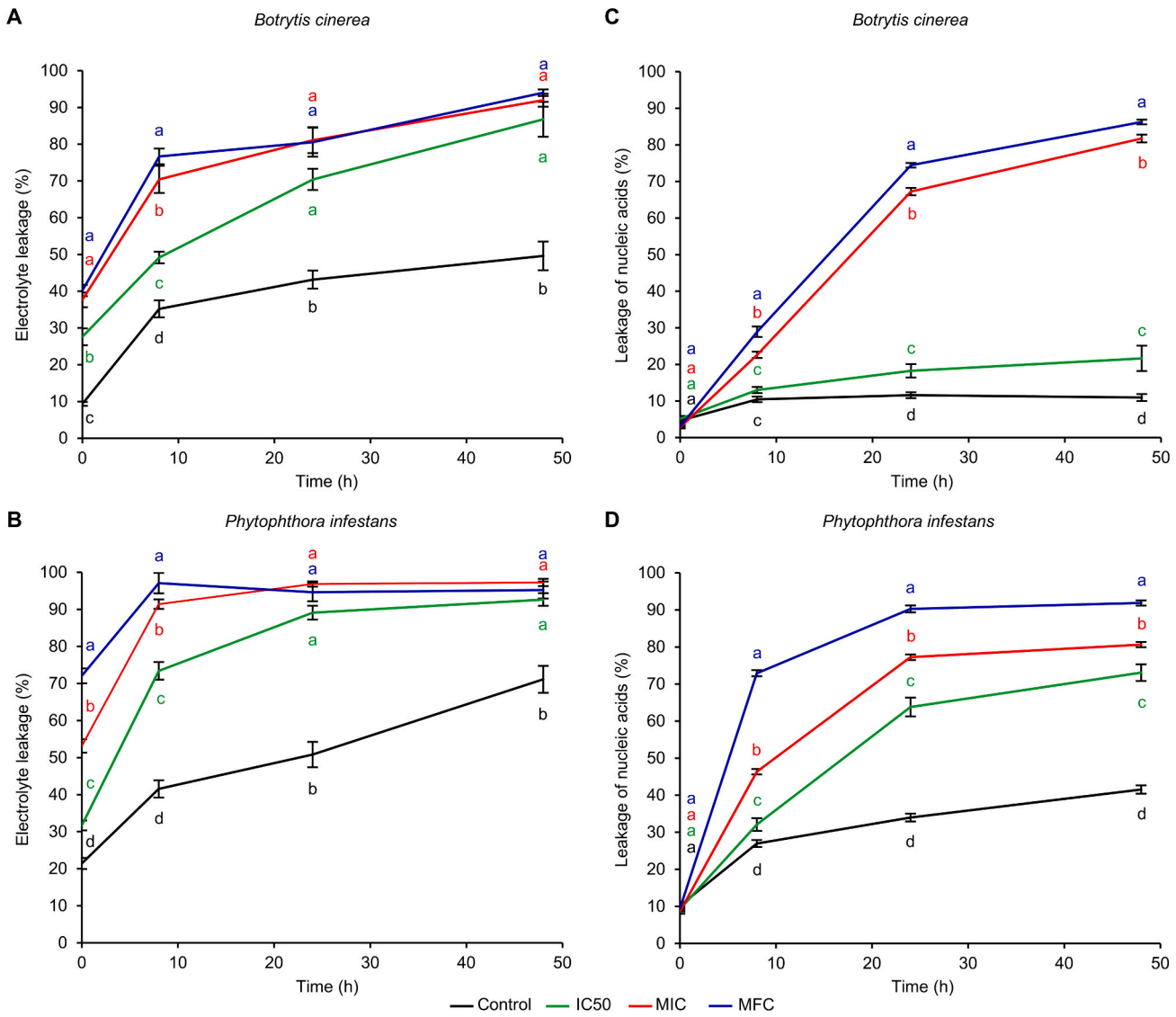

Fig. 2. Choline pelargonate increased membrane permeability of *B. cinerea* and *P. infestans* . The leakage of electrolytes (A, B) and nucleic acids (B, C) of *B. cinerea* and *P. infestans* mycelia was assessed at different time points (h) after incubation in distilled water supplemented or not (Control, black) with choline pelargonate at the concentration that inhibited 50 % of mycelial growth (IC50; green), minimum inhibitory concentration (MIC, red), and minimum fungicidal concentration (MFC, blue). Comparable results were obtained between the two experiments (Kruskal-Wallis $P > 0.05$, six replicates per experiment), and data were pooled. Mean and standard error values of twelve replicates (tubes) from the two experiments are presented for each treatment. For each time point, different letters indicate significant differences among treatments, according to the Kruskal-Wallis test followed by the Conovan-Iman test ($P \leq 0.05$). (For interpretation of the references to colour in this figure legend, the reader is referred to the web version of this article.)

in *P. infestans* TAG (Fig. 6A). Moreover, FFA (9:0) (pelargonic acid) was found in CP-treated *P. infestans* mycelia and the content of FFA (16:0), FFA (18:0), FFA (18:1), and FFA (20:1) was higher in CP-treated (MFC dosage) compared to control samples, as possible impacts of CP on lipid metabolism (Fig. 6B).

4. Discussion

CP is an organic salt of pelargonic acid belonging to the choline carboxylate class, which includes molecules with a hydrophilic choline head and a lipophilic acyl chain of variable length (Rengstl et al., 2014). Here, we found that CP can inhibit mycelial growth and spore germination of *B. cinerea* and *P. infestans* with dose-dependent effects *in vitro*. In particular, the IC50 and MFC of CP were 0.4 mM and 2.0 mM for *B. cinerea* mycelia, 0.3 mM and 5.0 mM for *P. infestans* mycelia, respectively. Slight germination of *B. cinerea* conidia and *P. infestans* sporangia was found at MFC dosage, suggesting a partial tolerance of spores compared to mycelia against CP. Choline carboxylates (e.g., choline derivatives of ethanoate, propanoate, butanoate, 2-methylpropanoate, pentanoate, 2,2-dimethylpropanoate, hexanoate, octanoate, and decanoate) are known to inhibit mycelial growth and spore germination of filamentous fungi, such as *Penicillium brevicompactum*, *P. corylophilum*, *P. diversum*, and *P. glandicola*, (Petkovic et al., 2010). Likewise, choline amino acids (e.g., choline derivatives of glycine, alanine, serine, threonine, isoleucine, methionine, phenylalanine, proline, and lysine) can inhibit bacterial growth of human pathogens, such as *Escherichia coli*, *Listeria monocytogenes*, *Salmonella enterica*, and *Staphylococcus aureus* (Hou et al., 2013). Moreover, pelargonic acid showed inhibitory activities against *S. enterica* subsp. *enterica* (Dev Kumar et al., 2020), *Microsporum gypseum* (Chadeganipour and Haims, 2001), and two cocoa pathogens, such as *Moniliophthora perniciosa* (formerly *Crinipellis perniciosa*) and *Moniliophthora roreri* (Aneja et al., 2005). Other carboxylic acids (e.g., butyric acid, caproic acid, caprylic acid, capric acid, lauric acid, and palmitic acid) can inhibit mycelial

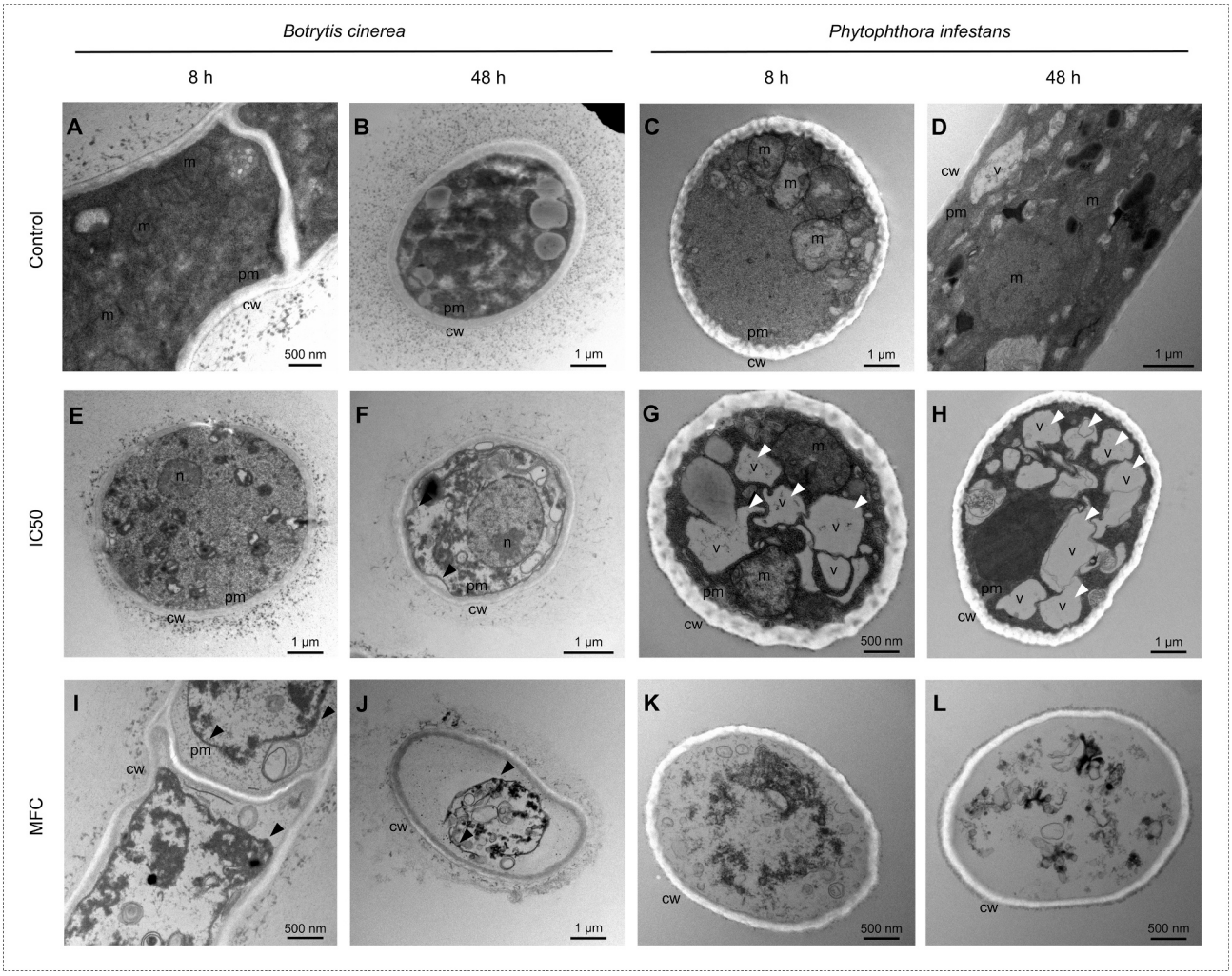

Fig. 3. Choline pelargonate altered *B. cinerea* and *P. infestans* ultrastructure. Transmission electron microscopy observations of *B. cinerea* and *P. infestans* mycelia were carried out after 8 h and 48 h of incubation in potato dextrose broth and pea broth supplemented or not (Control; A-D) with choline pelargonate at the concentration that inhibited 50 % of mycelial growth (IC50; *E*-H) and minimum fungicidal concentration (MFC; I-L). Three replicates were analyzed for each treatment. A representative picture is reported for each treatment and time point. Abbreviations: cw, cell wall; pm, plasma membrane; n, nucleus; m, mitochondria; v, vacuole. Black arrows indicate the plasma membrane detachment from the cell wall (shrunken cytoplasm and plasmolysis), and white arrows indicate intense vacuolization.

growth and spore germination of fungal phytopathogens, such as *Alternaria solani*, *Colletotrichum lagenarium*, *Fusarium oxysporum* f. sp. *cucumerinum*, and *F. oxysporum* f. sp. *lycopersici* (Liu et al., 2008), suggesting the key contribution of the lipophilic chain to the antimicrobial activity of choline carboxylates. In particular, choline carboxylates with a chain length of more than eight carbon atoms (e.g., choline pelargonate and choline decanoate) can interact with the bilayer membrane of liposomes, and their cytotoxicity on human cell lines increases with increased carbon chain length, although these cytotoxicity levels are very low and considered harmless for humans (Rengstl et al., 2014). A correlation between the lipophilicity and toxicity of choline carboxylates and choline amino acids was observed against fungi (Petkovic et al., 2010) and bacteria (Hou et al., 2013), suggesting a mechanism of action based on the interaction with cell membranes. In our analyses, CP treatment caused the leakage of electrolytes and nucleic acids from *B. cinerea* and *P. infestans* mycelia, indicating the disruption of cell membrane functionality. Ultrastructure analyses revealed severe plasma membrane perturbation, cytoplasmic shrinkage, plasmolysis, cytoplasm disorganization, and intense vacuolization in CP-treated *B. cinerea* and *P. infestans* cells, corroborating the negative impacts of CP on cell membrane structure. Shrunken and disorganized cytoplasm was previously associated with plasma membrane perturbation in *C. albicans* cells treated with FFA (e.g., capric acid and lauric acid) (Bergsson et al., 2001). Similar ultrastructure alterations (cytoplasm disorganization, cytoplasmic shrinkage, membrane disruption, and vacuolization) were also previously found in *B. cinerea* cells treated with sulfonamide fungicides, such as 1S,2R-((3-bromophenethyl)amino)-N-(4-chloro-2-trifluoromethylphenyl)cyclohexane-1-sulfonamide (Peng et al., 2020) and N-(2-trifluoromethyl-4-chlorphenyl)-2-oxocyclohexyl-sulfonamide (Yan et al., 2022), and in *P. infestans* cells treated with a pyrimidinamine fungicide (SYP-34773) (Wang et al., 2021) or cyclic lipopeptide (iturin A) (Wang et al., 2020). Cytoplasm disorganization, plasmolysis, and vacuolization were also observed in *B. cinerea* treated with essential oils of tea tree (Shao et al., 2013), *Cymbopogon citratus*, *Thymus vulgraris*, and *Origanum heracleoticum* (Yan et al., 2021). Similarly, *Phytophthora* spp. cells treated with essential oils showed severe alterations of the plasma membrane and cytoplasmic content, such as *P. capsici* treated with zedoary turmeric oil (Wang et al., 2019) and *P. cactorum* treated with methyleugenol (Dan et al., 2010). The inhibitory activity of essential oils against *B. cinerea* and *Phytophthora* spp. was associated with their lipophilic character (Dan et al., 2010; Shao et al., 2013; Wang et al., 2019; Yan et al., 2021), supporting that partially lipophilic molecules, such as

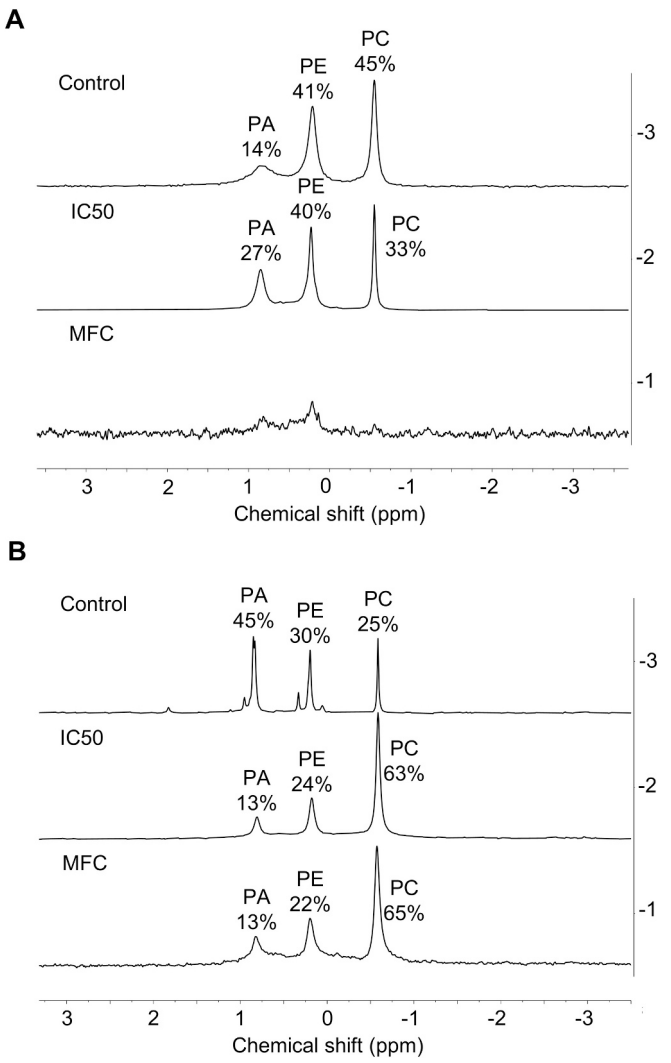

Fig. 4. Choline pelargonate changed the phospholipid content of *B. cinerea* and *P. infestans*. Nuclear magnetic resonance (NMR) spectra of *B. cinerea* (A) and *P. infestans* (B) lipids were obtained after 48 h of incubation in distilled water supplemented or not (Control) with choline pelargonate at the concentration that inhibited 50 % of mycelial growth (IC50) and minimum fungicidal concentration (MFC). Lipid classes of phosphatidic acid (PA), phosphatidylcholine (PC), and phosphatidylethanolamine (PE) were identified through comparisons with previous NMR measurements carried out with commercially available lipid standards. The molar fraction (percentage) of each lipid class was assessed according to peak integration.

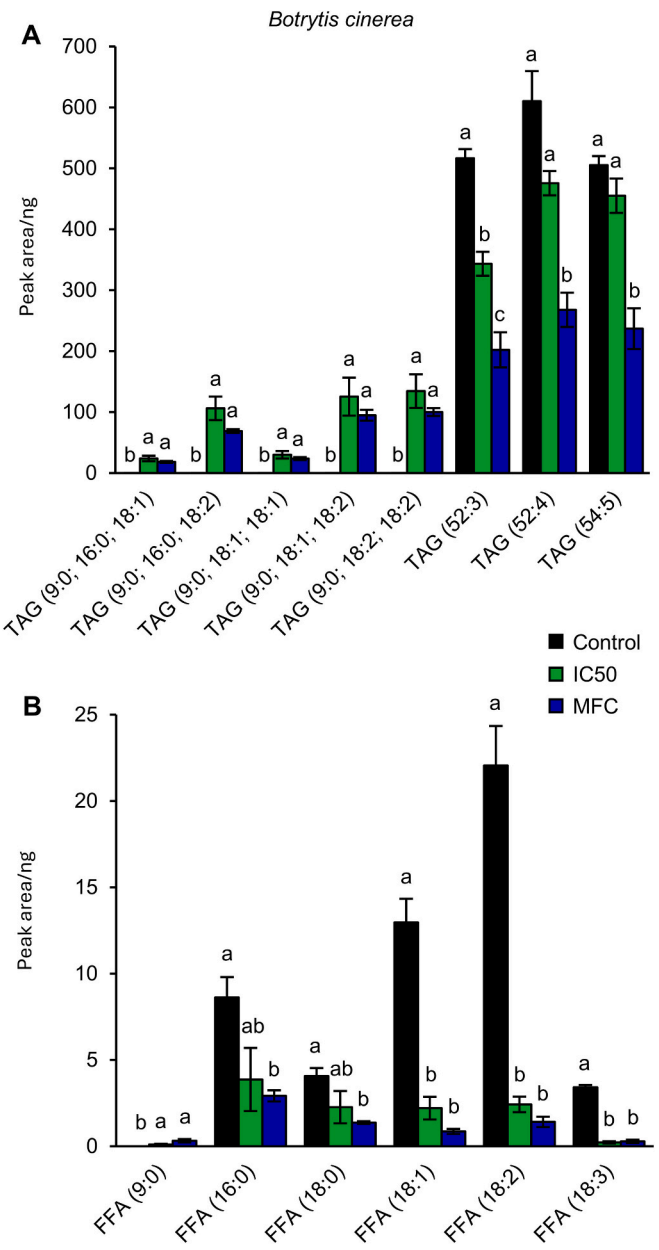

Fig. 5. Choline pelargonate changed the lipid content of *B. cinerea*. The content of triglycerides (TAG, A) and free fatty acids (FFA, B) of *B. cinerea* mycelia was analyzed by high-performance liquid chromatography-mass spectrometry (HPLC-MS) after 48 h of incubation in distilled water supplemented or not (Control, black) with choline pelargonate at the concentration that inhibited 50 % of mycelial growth (IC50; green) and minimum fungicidal concentration (MFC; blue). Lipid content was expressed as peak area per ng of dried lipid extract (peak area/ng). Mean and standard error values of three replicates (tubes) are presented for each treatment. Non-detectable values were considered as zero values. For each lipid (named according to the number of carbon atoms and unsaturated bonds reported in brackets), different letters indicate significant differences among treatments, according to the Kruskal-Wallis test followed by the Conovan-Iman test ($P \leq 0.05$). Most abundant TAG (> 500 peak area/ng), TAG containing a 9:0 carbon chain, and all FFA detected in *B. cinerea* are shown. Less abundant TAG showed a profile comparable to TAG (52:3), such as TAG (52:2), TAG (54:2), and TAG (54:4). (For interpretation of the references to colour in this figure legend, the reader is referred to the web version of this article.)

CP, can interact with cell membranes and perturb their integrity and functionality, with severe impacts on cell ultrastructure and vitality.

Ultrastructure alterations in response to antimicrobial compounds were previously associated with changes in the lipid composition of cell membranes in *B. cinerea* (Shao et al., 2013) and *P. capsici* (Ma et al., 2021). Phospholipids (e.g., PA, PC, and PE) are the main components of cell membranes in eukaryotic cells (Morita and Ikeda, 2022), and their molar fraction was altered by CP treatment in *B. cinerea* and *P. infestans* mycelia. In particular, the content of PA [e.g., PA (36:3), PA (36:4), PA (36:5), PA (36:6), and PA (38:3)], PC [e.g., PC (34:1), PC (34:2), PC (34:3), PC (34:4), PC (36:2), PC (36:3), PC (36:4), PC (36:5), and PC (36:6)], and PE [e.g., PE (34:2), PE (36:3), and PE (36:4)] was lower in CP-treated compared to control *B. cinerea* mycelia. Likewise, the content of PC (e.g., lecithin) and PE (e.g., cephalin) of *B. cinerea* mycelia was lowered by treatments with flavonoids from *Sedum aizoon* (Wang et al., 2023). The content of TAG [e.g., TAG(52:3), TAG(52:4), and TAG(54:5)] and FFA [e.g., FFA(16:0), FFA(18:0), FFA(18:1), FFA(18:2), and FFA

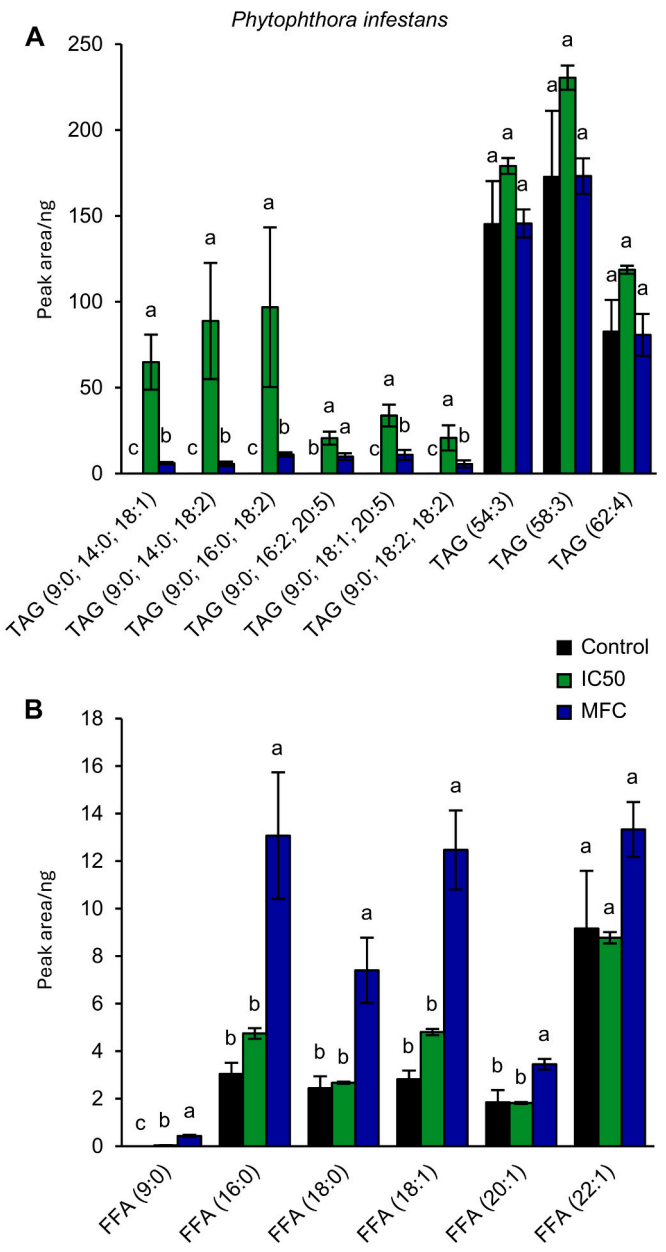

Fig. 6. Choline pelargonate changed the lipid content of *P. infestans*. The content of triglycerides (TAG, A) and free fatty acids (FFA, B) of *P. infestans* mycelia was analyzed by high-performance liquid chromatography-mass spectrometry (HPLC-MS) after 48 h of incubation in distilled water supplemented or not (Control, black) with choline pelargonate at the concentration that inhibited 50 % of mycelial growth (IC50; green) and minimum fungicidal concentration (MFC; blue). Lipid content was expressed as peak area per ng of dried lipid extract (peak area/ng). Mean and standard error values of three replicates (tubes) are presented for each treatment. Non-detectable values were considered as zero values. For each lipid (named according to the number of carbon atoms and unsaturated bonds reported in brackets), different letters indicate significant differences among treatments, according to the Kruskal-Wallis test followed by the Conovan-Iman test ($P \leq 0.05$). Most abundant TAG (> 80 peak area/ng), TAG containing a 9:0 carbon chain, most abundant FFA (> 1.8 peak area/ng), and FFA containing a 9:0 carbon chain detected in *P. infestans* are shown. The content of less abundant TAG was not affected by CP treatment, such as TAG (52:7), TAG (56:9), and TAG (60:15). Less abundant FFA showed a profile comparable to FFA (16:0) [e.g., FFA (18:2) and FFA (20:3)] or FFA (22:1) [e.g., FFA (20:5) and FFA (24:1)]. (For interpretation of the references to colour in this figure legend, the reader is referred to the web version of this article.)

(18:3)] decreased in CP-treated *B. cinerea* mycelia, indicating that CP can perturb lipid metabolism and stimulate the hydrolysis of membrane lipids. Likewise, FFA content [e.g. palmitic acid, FFA (16:0); stearic acid, FFA (18:0); oleic acid, FFA (18:1); linoleic acid, FFA (18:2); and linolenic acid, FFA (18:3)] of *B. cinerea* can change in response to tea tree oil treatment (Shao et al., 2013), and *B. cinerea* genes involved in the lipid metabolism can be modulated in response to treatments with flavonoids from *S. aizoon* (Wang et al., 2022), corroborating that toxicity of lipophilic molecules can be associated with increases in membrane permeability and changes in the lipid metabolism and lipid content. In *P. infestans*, the CP-dependent perturbation of cell membranes was associated with decreased PA molar fraction, increased PC molar fraction, and slight changes in PE molar fraction. In particular, the content of PC (34:1), PC (34:2), PC (36:2), PC (36:3), PC (38:6), and PE (34:1) increased in CP-treated compared to control *P. infestans* mycelia, while the content of PE (40:10) decreased. Moreover, the content of FFA (16:0), FFA (18:0), FFA (18:1), FFA (20:1), PA (38:5), and PA (38:6) was higher in CP-treated compared to control *P. infestans* mycelia, while the content of PA (38:8), PA (38:9), PA (40.9), TAG (54:3) TAG (58:3), and TAG (62:4) was comparable in CP-treated and control samples, suggesting a complex perturbation of lipid metabolism in *P. infestans* mycelia. Likewise, changes in the content of membrane lipids were previously found in *P. sojae* mycelia treated with a fungicide (oxathiapiprolin) (Liu et al., 2023) and *P. capsici* treated with a chitosan-copper complex (Ma et al., 2021), indicating that perturbation of membrane structure and functionality in *Phytophthora* spp. is associated to changes of lipid metabolism and hydrolysis of membrane lipids. Moreover, CP treatment increased the content of pelargonic acid [FFA (9:0)] and TAG possibly derived from pelargonic acid incorporation in *B. cinerea* mycelia [e.g., TAG (9:0; 16:0; 18:1), TAG (9:0; 16:0; 18:2), TAG (9:0; 18:1; 18:1), TAG (9:0; 18:1; 18:2), and TAG (9:0; 18:2; 18:2)] and *P. infestans* mycelia [e.g., TAG (9:0;14:0; 18:1), TAG (9:0; 14:0; 18:2), TAG (9:0; 16:0; 18:2), TAG (9:0; 16:2; 20:5), TAG (9:0; 18:1; 20:5), and TAG (9:0; 18:2; 18:2)]. The incorporation of pelargonic acid in TAG lipids could represent an attempted detoxification mechanism activated in response to lipophilic molecules, as previously hypothesized by the increase of lipid content in *B. cinerea* cells treated with methyl cis-7-oxodeisopropyldehydroabietate (Feio et al., 2002). The *in vitro* characterization of the mode of action revealed high inhibitory activities and severe impacts of CP against *B. cinerea* and *P. infestans* cells, but further studies are required to verify the efficacy of CP against plant diseases under controlled and field conditions and to verify possible side effects on the community of plant-associated microorganisms.

5. Conclusions

CP inhibited mycelial growth and spore germination of *B. cinerea* and *P. infestans* and caused the leakage of cytoplasmic content in both phytopathogens *in vitro*. Severe ultrastructural alterations were observed in *B. cinerea* and *P. infestans* cells with the perturbation of lipid content, suggesting negative impacts of CP on cell membrane structure and functionality. However, CP effects on lipid content differed in *B. cinerea* and *P. infestans* mycelia, suggesting specific responses to this choline carboxylate in the two phytopathogens. CP is a promising sustainable fungicide against phytopathogens, and further studies are required to verify the efficacy of CP against plant diseases under controlled and field conditions.

Author contribution

SM and AN analyzed the antifungal activity and electrolyte leakage. SM, FT, and GG analyzed the lipid content. LL, and BB carried out the ultrastructure observations. MP, CL, and SM conceived the study and designed the experiments. SM and MP wrote the manuscript. All the authors revised and approved the final manuscript.

CRediT authorship contribution statement

Sofia Montanari: Writing – original draft, Investigation, Data curation. **Francesco Trenti:** Writing – original draft, Investigation, Data curation. **Andrea Nesler:** Writing – review & editing, Supervision, Investigation, Conceptualization. **Lorella Navazio:** Writing – review & editing, Supervision, Data curation. **Barbara Baldan:** Writing – review & editing, Supervision, Data curation. **Graziano Guella:** Writing – review & editing, Supervision, Data curation. **Claudia M.O. Longa:** Investigation. **Michele Perazzolli:** Writing – review & editing, Writing – original draft, Supervision, Funding acquisition, Data curation.

Declaration of competing interest

AN is employed by Bi-PA nv. The remaining authors declare no conflict of interest.

Acknowledgments

We thank Silvia Moschin and Elisabetta Offer (University of Padova) for technical support and the Imaging Facility of the Department of Biology, University of Padova, for assistance with transmission electron microscopy analyses. Ultrastructure analyses were supported by the Italian Ministry of University (PRIN2022 grant no. 2022NW97JX). Data interpretation was supported by the SCALE-it project (101181496) co-funded by the Horizon Europe programme under the call HORIZON-CL6-2024FARM2FORK-02 and the Swiss State Secretariat for Education, Research and Innovation (SERI).

Appendix A. Supplementary data

Supplementary data to this article can be found online at https://doi.org/10.1016/j.pestbp.2025.106471.

References

Abbey, J.A., Percival, D., Abbey, L., Asiedu, S.K., Prithiviraj, B., Schilder, A., 2019. Biofungicides as alternative to synthetic fungicide control of grey mould (*Botrytis cinerea*) – prospects and challenges. Biocontrol Sci. Tech. 29, 207–228.

Amselem, J., Cuomo, C.A., van Kan, J.A., Viaud, M., Benito, E.P., Couloux, A., Coutinho, P.M., de Vries, R.P., Dyer, P.S., Fillinger, S., Fournier, E., Gout, L., Hahn, M., Kohn, L., Lapalu, N., Plummer, K.M., Pradier, J.M., Quévillon, E., Sharon, A., Simon, A., ten Have, A., Tudzynski, B., Tudzynski, P., Wincker, P., Andrew, M., Anthouard, V., Beever, R.E., Beffa, R., Benoit, I., Bouzid, O., Brault, B., Chen, Z., Choquer, M., Collémare, J., Cotton, P., Danchin, E.G., Da Silva, C., Gautier, A., Giraud, C., Giraud, T., Gonzalez, C., Grossetete, S., Güldener, U., Henrissat, B., Howlett, B.J., Kodira, C., Kretschmer, M., Lappartient, A., Leroch, M., Levis, C., Mauceli, E., Neuvéglise, C., Oeser, B., Pearson, M., Poulain, J., Poussereau, N., Quesneville, H., Rascle, C., Schumacher, J., Ségurens, B., Sexton, A., Silva, E., Sirven, C., Soanes, D.M., Talbot, N.J., Templeton, M., Yandava, C., Yarden, O., Zeng, Q., Rollins, J.A., Lebrun, M.H., Dickman, M., 2011. Genomic analysis of the necrotrophic fungal pathogens *Sclerotinia sclerotiorum* and *Botrytis cinerea*. PLoS Genet. 7, e1002230.

Aneja, M., Gianfagna, T.J., Hebbar, P.K., 2005. *Trichoderma harzianum* produces nonanoic acid, an inhibitor of spore germination and mycelial growth of two cacao pathogens. Physiol. Mol. Plant Pathol. 67, 304–307.

Baccelli, I., Luti, S., Bernardi, R., Favaron, F., De Zotti, M., Sella, L., 2022. Water-soluble trichogin ga iv-derived peptaibols protect tomato plants from *Botrytis cinerea* infection with limited impact on plant defenses. Front. Plant Sci. 13.

Bergsson, G., Arnfinnsson, J., Steingrímsson, Ó., Thormar, H., 2001. *In vitro* killing of *Candida albicans* by fatty acids and monoglycerides. Antimicrob. Agents Chemother. 45, 3209–3212.

Chadeganipour, M., Haims, A., 2001. Antifungal activities of pelargonic and capric acid on *Microsporum gypseum*. Mycoses 44, 109–112.

Chahed, A., Nesler, A., Navazio, L., Baldan, B., Busato, I., Ait Barka, E., Pertot, I., Puopolo, G., Perazzolli, M., 2020. The rare sugar tagatose differentially inhibits the growth of *Phytophthora infestans* and *Phytophthora cinnamomi* by interfering with mitochondrial processes. Front. Microbiol. 11, 128.

Chen, C., Wan, C., Peng, X., Chen, J., 2020. A flavonone pinocembroside inhibits *Penicillium italicum* growth and blue mold development in 'Newhall' navel oranges by targeting membrane damage mechanism. Pestic. Biochem. Physiol. 165, 104505.

Cheung, N., Tian, L., Liu, X., Li, X., 2020. The destructive fungal pathogen *Botrytis cinerea*—insights from genes studied with mutant analysis. Pathogens 9, 923.

Ciriminna, R., Fidalgo, A., Ilharco, L.M., Pagliaro, M., 2019. Herbicides based on pelargonic acid: herbicides of the bioeconomy. Biofuels Bioprod. Biorefin. 13, 1476–1482.

Commission, E, 2015. List of Candidates for Substitution (January 2015), Commission Implementing Regulation (EU) 2015/408 of 11 March 2015 on Implementing Article 80(7) of Regulation (EC) No 1107/2009 of the European Parliament. https://eur-lex.europa.eu/legal-content/EN/TXT/PDF/?uri=CELEX:32015R0408.

Commission, E, 2018. Commission implementing regulation (EU) 2018/1981 of 13 December 2018 renewing the approval of the active substances copper compounds, as candidates for substitution, in accordance with regulation (EC) no 1107/2009 of the European Parliament and of the council concerning the placing of plant protection products on the market, and amending the annex to commission implementing regulation (EU) No 540/2011. O. J. Eur. Union L317, 16–18. https://www.legislation.gov.uk/cy/eur/2018/1981.

Dan, Y., Liu, H.-Y., Gao, W.-W., Chen, S.-L., 2010. Activities of essential oils from *Asarum heterotropoides* var. *mandshuricum* against five phytopathogens. Crop Prot. 29, 295–299.

De Saegher, J., Nguyen, H.N., Frati, S., Nesler, A., Vermaete, A., 2019. Composition Comprising a Choline Salt of a Fatty Acid and the Use Thereof as a Fungicide. WO2020104645A1 (BE1026309B1).

Dev Kumar, G., Mis Solval, K., Mishra, A., Macarisin, D., 2020. Antimicrobial efficacy of pelargonic acid micelles against *Salmonella* varies by surfactant, serotype and stress response. Sci. Rep. 10, 10287.

Elhi, F., Gantman, M., Nurk, G., Schulz, P.S., Wasserscheid, P., Aabloo, A., Põhako-Esko, K., 2020. Influence of carboxylate anions on phase behavior of choline ionic liquid mixtures. Molecules 25, 1691.

Feio, S.S., Franca, S., Silva, A.M., Gigante, B., Roseiro, J.C., Marcelo Curto, M.J., 2002. Antimicrobial activity of methyl cis-7-oxo deisopropyldehydroabietate on *Botrytis cinerea* and *Lophodermium seditiosum*: ultrastructural observations by transmission electron microscopy. J. Appl. Microbiol. 93, 765–771.

Folch, J., Lees, M., Stanley, G.H.S., 1957. A simple method for the isolation and purification of total lipides from animal tissues. J. Biol. Chem. 226, 497–509.

Haverkort, A.J., Struik, P.C., Visser, R.G.F., Jacobsen, E., 2009. Applied biotechnology to combat late blight in potato caused by *Phytophthora infestans*. Potato Res. 52, 249–264.

Hou, X.-D., Liu, Q.-P., Smith, T.J., Li, N., Zong, M.-H., 2013. Evaluation of toxicity and biodegradability of cholinium amino acids ionic liquids. PLoS One 8, e59145.

Ivanov, A.A., Ukladov, E.O., Golubeva, T.S., 2021. *Phytophthora infestans*: an overview of methods and attempts to combat late blight. J. Fungi. 7, 1071.

Judelson, H.S., 2014. Phytophthora infestans. In: Dean, R.A., Lichens-Park, A., Kole, C. (Eds.), Genomics of Plant-Associated fungi and Oomycetes: Dicot Pathogens. Springer, Berlin Heidelberg, Berlin, Heidelberg, pp. 175–208.

Judelson, H.S., Blanco, F.A., 2005. The spores of *Phytophthora*: weapons of the plant destroyer. Nat. Rev. Microbiol. 3, 47–58.

Leroux, P., 2007. Chemical control of *Botrytis* and its resistance to chemical fungicides. In: Elad, Y., Williamson, B., Tudzynski, P., Delen, N. (Eds.), *Botrytis*: Biology, Pathology and Control. Springer, Netherlands, Dordrecht, pp. 195–222.

Li, X., Zhang, Y., Wei, Z., Guan, Z., Cai, Y., Liao, X., 2016. Antifungal activity of isolated *Bacillus amyloliquefaciens* SYBC H47 for the biocontrol of peach gummosis. PLoS One 11, e0162125.

Li, X., Ma, N., Zhang, L., Ling, G., Zhang, P., 2022. Applications of choline-based ionic liquids in drug delivery. Int. J. Pharm. 612, 121366.

Liu, S., Ruan, W., Li, J., Xu, H., Wang, J., Gao, Y., Wang, J., 2008. Biological control of phytopathogenic fungi by fatty acids. Mycopathologia 166, 93–102.

Liu, X., Li, C., Chen, Y., Xue, Z., Miao, J., Liu, X., 2023. Untargeted lipidomics reveals lipid metabolism disorders induced by oxathiapiprolin in *Phytophthora sojae*. Pest Manag. Sci. 79, 1593–1603.

Ma, Y., Gao, K., Yu, H., Liu, W., Qin, Y., Xing, R., Liu, S., Li, P., 2021. C-coordinated O-carboxymethyl chitosan Cu(II) complex exerts antifungal activity by disrupting the cell membrane integrity of *Phytophthora capsici* Leonian. Carbohydr. Polym. 261, 117821.

Mazumdar, P., Singh, P., Kethiravan, D., Ramathani, I., Ramakrishnan, N., 2021. Late blight in tomato: insights into the pathogenesis of the aggressive pathogen *Phytophthora infestans* and future research priorities. Planta 253, 119.

Morita, S.-Y., Ikeda, Y., 2022. Regulation of membrane phospholipid biosynthesis in mammalian cells. Biochem. Pharmacol. 206, 115296.

Novak, M., Krpan, T., Panevska, A., Shewell, L.K., Day, C.J., Jennings, M.P., Guella, G., Sepčić, K., 2020. Binding specificity of ostreolysin A6 towards Sf9 insect cell lipids. Biochim. Biophys. Acta Biomembr. 1862, 183307.

Nowicki, M., Foolad, M.R., Nowakowska, M., Kozik, E.U., 2012. Potato and tomato late blight caused by *Phytophthora infestans*: an overview of pathology and resistance breeding. Plant Dis. 96, 4–17.

Peng, J., Wang, K., Feng, T., Zhang, H., Li, X., Qi, Z., 2020. The effect of (1S,2R-((3-bromophenethyl)amino)-N-(4-chloro-2-trifluoromethylphenyl) cyclohexane-1-sulfonamide) on *Botrytis cinerea* through the membrane damage mechanism. Molecules 25, 94.

Penry, J.T., Manore, M.M., 2008. Choline: an iportant micronutrient for maximal endurance-exercise performance? Int. J. Sport Nutr. Exerc. Metab. 18, 191–203.

Petkovic, M., Ferguson, J.L., Gunaratne, H.Q.N., Ferreira, R., Leitão, M.C., Seddon, K.R., Rebelo, L.P.N., Pereira, C.S., 2010. Novel biocompatible cholinium-based ionic liquids—toxicity and biodegradability. Green Chem. 12, 643–649.

Puopolo, G., Cimmino, A., Palmieri, M.C., Giovannini, O., Evidente, A., Pertot, I., 2014. *Lysobacter capsici* AZ78 produces cyclo(l-Pro-l-Tyr), a 2,5-diketopiperazine with toxic activity against sporangia of *Phytophthora infestans* and *Plasmopara viticola*. J. Appl. Microbiol. 117, 1168–1180.

Rengstl, D., Kraus, B., Van Vorst, M., Elliott, G.D., Kunz, W., 2014. Effect of choline carboxylate ionic liquids on biological membranes. Colloids Surf. B: Biointerfaces 123, 575–581.
Shao, X., Cheng, S., Wang, H., Yu, D., Mungai, C., 2013. The possible mechanism of antifungal action of tea tree oil on *Botrytis cinerea*. J. Appl. Microbiol. 114, 1642–1649.
Skevas, T., Oude Lansink, A.G.J.M., Stefanou, S.E., 2013. Designing the Emerging EU Pesticide Policy: A Literature Review, 64-65, pp. 95–103.
Song, Y., He, L., Chen, L., Ren, Y., Lu, H., Geng, S., Mu, W., Liu, F., 2016. Baseline sensitivity and control efficacy of antibiosis fungicide tetramycin against *Botrytis cinerea*. Eur. J. Plant Pathol. 146, 337–347.
Tamm, L., Thuerig, B., Apostolov, S., Blogg, H., Borgo, E., Corneo, P.E., Fittje, S., de Palma, M., Donko, A., Experton, C., Alcázar Marín, É., Morell Pérez, Á., Pertot, I., Rasmussen, A., Steinshamn, H., Vetemaa, A., Willer, H., Herforth-Rahmé, J., 2022. Use of copper-based fungicides in organic agriculture in twelve European countries. Agronomy 12, 673.
Tleuova, A.B., Wielogorska, E., Talluri, V.S.S.L.P., Štěpánek, F., Elliott, C.T., Grigoriev, D. O., 2020. Recent advances and remaining barriers to producing novel formulations of fungicides for safe and sustainable agriculture. J. Control. Release 326, 468–481.
Wang, B., Liu, F., Li, Q., Xu, S., Zhao, X., Xue, P., Feng, X., 2019. Antifungal activity of zedoary turmeric oil against *Phytophthora capsici* through damaging cell membrane. Pestic. Biochem. Physiol. 159, 59–67.
Wang, Y., Zhang, C., Liang, J., Wu, L., Gao, W., Jiang, J., 2020. Iturin a extracted from *Bacillus subtilis* WL-2 affects *Phytophthora infestans* via cell structure disruption, oxidative stress, and energy supply dysfunction. Front. Microbiol. 11.
Wang, W., Liu, Y., Xue, Z., Li, J., Wang, Z., Liu, X., 2021. Activity of the novel gungicide SYP-34773 against plant pathogens and its mode of action on *Phytophthora infestans*. J. Agric. Food Chem. 69, 11794–11803.
Wang, K., Zhang, X., Shao, X., Wei, Y., Xu, F., Wang, H., 2022. Flavonoids from *Sedum aizoon* L. inhibit *Botrytis cinerea* by negatively affecting cell membrane lipid metabolism. Appl. Microbiol. Biotechnol. 106, 7139–7151.
Wang, K., Ge, Q., Shao, X., Wei, Y., Zhang, X., Xu, F., Wang, H., 2023. Influences of flavonoids from *Sedum aizoon* L. on the cell membrane of *Botrytis cinerea*. Food Biosci. 52, 102386.
Williamson, B., Tudzynski, B., Tudzynski, P., Van Kan, J.A.L., 2007. *Botrytis cinerea*: the cause of grey mould disease. Mol. Plant Pathol. 8, 561–580.
Yahyazadeh, M., Omidbaigi, R., Zare, R., Taheri, H., 2008. Effect of some essential oils on mycelial growth of *Penicillium digitatum* Sacc. World J. Microbiol. Biotechnol. 24, 1445–1450.
Yan, J., Wu, H., Chen, K., Feng, J., Zhang, Y., 2021. Antifungal activities and mode of action of *Cymbopogon citratus*, *Thymus vulgaris*, and *Origanum heracleoticum* essential oil vapors against *Botrytis cinerea* and their potential application to control postharvest strawberry gray mold. Foods 10, 2451.
Yan, X., Chen, S., Sun, W., Zhou, X., Yang, D., Yuan, H., Wang, D., 2022. Primary mode of action of the novel sulfonamide fungicide against *Botrytis cinerea* and field control effect on tomato gray mold. Int. J. Mol. Sci. 23, 1526.
Yuen, J., 2021. Pathogens which threaten food security: *Phytophthora infestans*, the potato late blight pathogen. Food Secur. 13, 247–253.
Zhang, J., Ma, S., Du, S., Chen, S., Sun, H., 2019. Antifungal activity of thymol and carvacrol against postharvest pathogens *Botrytis cinerea*. J. Food Sci. Technol. 56, 2611–2620.
Zuppini, A., Gerotto, C., Baldan, B., 2010. Programmed cell death and adaptation: two different types of abiotic stress response in a unicellular chlorophyte. Plant Cell Physiol. 51, 884–895.